Geoenvironmental Disasters

RESEARCH

Open Access

Assessing tsunami vertical evacuation processes based on probabilistic tsunami hazard assessment for west coast of Aceh Besar, Indonesia

Ibrahim[1,2,3], Syamsidik[1,2,4*], Azmeri[1,4], Muttaqin Hasan[1,4], Abdullah Irwansyah[3] and Muhammad Daffa Al Farizi[2,4]

Abstract

Background Tsunamis are rare events compared to other disasters but have devastating consequences. In the last 100 years, more than 24 tsunamis and more than 235,000 fatalities have occurred globally. Indonesia has a high risk of a tsunami disaster. Since the devastating 2004 tsunami in the Indian Ocean, much research and preparatory work have been done to reduce the impact of future tsunamis in Indonesia, including in the province of Aceh, especially along the western coast where West Aceh is located. This coastal area was destroyed by a tsunami as high as 15–30 m, resulting in the loss of life, housing, tourist areas, industrial areas, and other public facilities. Given that tsunami disasters are rare and sometimes occur long in advance, human memory and awareness are reduced, making research on the level of tsunami awareness of disasters a challenging task.

Method Probabilistic Tsunami Hazard Assessment (PTHA) is a method that has been developed to predict tsunami hazards with a return period of hundreds to thousands of years, beyond the limited availability of historical data. The PTHA method can provide important information that supports tsunami risk management measures. This study aims to estimate recurrence period-based tsunami risk on the west coast of the district of Aceh Besar using the PTHA method. In this study, the source of the tsunami is caused by fault activity at sea. Seven tsunami scenarios based on fault parameters (earthquakes of magnitudes Mw 8.0 to 9.2 with interval 0,2) with the fault location focusing on the Aceh-Andaman Mega Thrust Segment, as applied in this study. This segment was a similar source to the 2004 Indian Ocean tsunami that created a rupture area along a distance of 1155 km, with six parts of the fault.

Result The maximum inundation distance reached 6 km for the flat area, with a flow depth of 13 m. The site has a cliff that is close to the shoreline, with an inundation distance shorter than the distance across the flat area. With an arrival time of less than 25 min, it is recommended to have an evacuation building and evacuation road in a wide inundated area, and an arrangement of hills close to the beach as an evacuation area, in order to reduce the number of casualties. For 100 years return period or exceedance probability rate 0.01, the average flow depth on the coast may exceed 5 m, and the maximum flow depth for a 1000-year return period or annual probability of 0.001 is 12 m. With the potential tsunami in the future, continuous tsunami drills and tsunami education are needed so that people can maintain an awareness of the threat posed by tsunamis.

Keywords Tsunami hazard, Probabilistic, Mitigation, Indonesia

*Correspondence:
Syamsidik
syamsidik@tdmrc.org; syamsidik@unsyiah.ac.id
Full list of author information is available at the end of the article

Introduction

Tsunamis are rare compared to other disasters, but tsunamis have devastating consequences (Grezio et al. 2017), and globally in the last century, there have been over 24 tsunamis and approximately 235,000 fatalities [UNISDR (The United Nations International Strategy for Disaster Reduction) 2013], notwithstanding the high threat for Indonesia. The history of tsunamis indicates that humanity has often been unprepared for disasters. Since the devastating 2004 tsunami in the Indian Ocean and the 2011 earthquake in East Japan were triggered, the whole world's awareness of the potentially disastrous consequences of tsunamis to coastal areas has increased, and also knowledge build and physical work to reduce the risk of future tsunamis have taken place (Goff and Terry 2012; Okal 2015; Frucht et al. 2021; Suppasri et al. 2021). Numerous tsunami-prone nations have implemented tsunami hazard assessment programmes to guide their risk reduction efforts.

Understanding tsunami risks as recurring events is still difficult for the population, and policy makers, policies and practices need to be integrated into Indonesian daily life. One of the reasons for the difficulty is the lack of support from sufficient studies that could convince disaster managers and practitioners to take note and act accordingly. There was one such study regarding probabilistic tsunami hazards in Indonesia, but it was conducted at the macro-scale with the aim of mapping all the coasts of Indonesia (Horspool et al. 2014) and was no connection with the local settings of the study area. Since that particular study, to our knowledge, there has not been another probabilistic-tsunami research undertaken in Indonesia (Sihombing and Torbol 2017). Hence, this resulted in the way tsunami risk has been perceived, in several official documents that are related to tsunami mitigation or preparedness at all levels. The probabilistic hazards analysis assumes that all events are unrelated to each other and follow the Poisson process or exponential patterns (Geist and Lynett 2014).

The north and northwestern coasts of Aceh were severely damaged by the earthquake and tsunami of December 26, 2004 (Al'ala et al. 2015; Syamsidik et al. 2016). Aceh is located on the island of Sumatra in the northern part, where the largest waves struck this area. The west coast of Aceh Besar, which is a district of the province of Aceh, was one of the locations destroyed by the 2004 Indian Ocean tsunami. The west coast of Aceh Besar is an area of residential, tourist, and industrial sectors (Fig. 1). In Lhoknga, one of the sub-districts of Aceh Besar, the town was entirely wiped out by a tsunami, except for one building that remains, the Mosque. Eighteen years after the tsunami, the community have rebuilt and currently thrive in the same place. In 2019, there were 31,412 people living in the study area, which comprised of three subdistricts named Lhoknga, Leupung, and Lhoong, with an annual population increase rate of 1.90 percent [Badan Pusat Statistik (BPS) 2019]. An essential challenge for government and researchers is to provide data, recommendations, and action to ensure that these communities are as safe as they can be.

In these zones, a study of tsunamis has been conducted for various reasons. The results of the 2004 tsunami simulation for the west coast of Aceh Besar, show the arrival time of the tsunami on the west coast of Aceh as 25–78 min (Syamsidik et al. 2015). Research on sediment transport, coastal erosion, and shoreline changes due to the tsunami has also been carried out by several previous researchers (NOAA; Paris et al. 2009; Gusman et al. 2012; Li et al. 2012; Ontowirjo et al. 2013; Satake et al. 2013; Siregar Novita 2016; Rasyif et al. 2016; Syamsidik et al. 2019). Jihad et al. (2020) stated that the zone of the west coast of Sumatra (a province of Indonesia), which includes the present study area, has a high risk of a tsunami occurring, and this is where all the components of the tsunami action plan should be implemented (Jihad et al. 2020). Recent research on the west coast of Aceh Besar is focused on the characteristics of the tsunami threat (Ibrahim et al. 2022). Since tsunami disasters are rare and sometimes they occurred a long time ago, human memory and awareness are reduced, making research on tsunami awareness levels a challenging task. Probabilistic Tsunami Hazard Assessment (PTHA) is a method developed to predict tsunami hazards with return periods of hundreds to thousands of years beyond the availability of limited historical data. The PTHA method will provide important information that supports tsunami hazard management measures. Various method can be implemented in tsunami hazard management measures such as fore dune regeneration and conservation, evacuation scenario, education, coastal ecosystem management and relocation (Martínez et al. 2020). PTHA methodology has been implemented in several locations of the world, and local, regional, and global PTHAs have been conducted to inform various policy choices (Grezio et al. 2017; Liu et al. 2021; Tonini et al. 2021).

This study aims to predict the long-term tsunami threat on the west coast of Aceh Besar using the PTHA method. In this study, the source of the tsunami is seafloor movement caused by an earthquake. However, PTHA can also be analysed for other causes of tsunamis, such as landslides, volcanic eruptions, and meteorites. Several tsunami scenarios based on fault parameters (earthquakes with magnitudes Mw 8.0 to 9.2) will be applied in this study. High-resolution topography was involved in tsunami inundation simulation

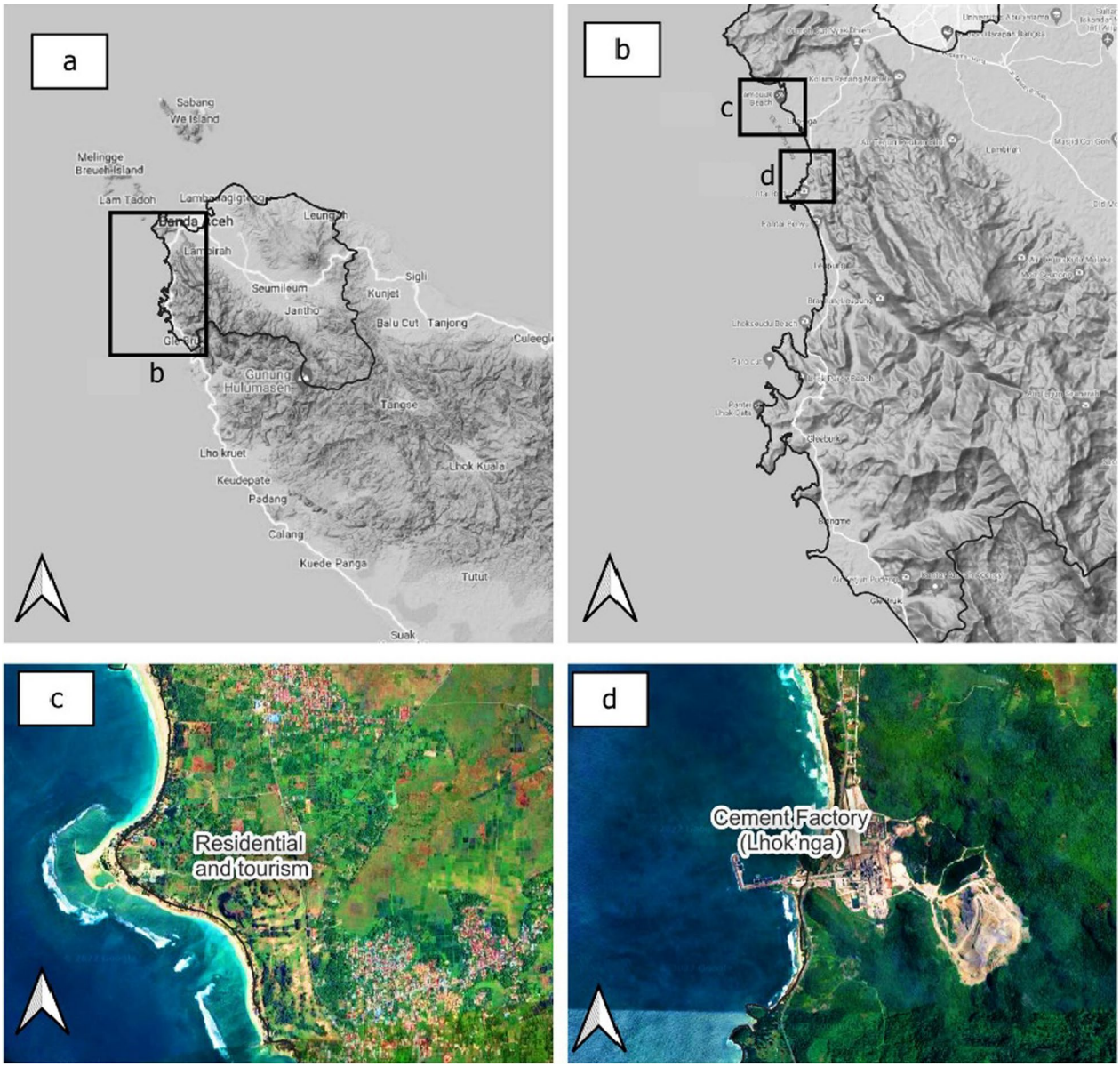

Fig. 1 Maps of the research area's location; **a** Aceh Province, **b** West coast of Aceh Besar, **c** residence and tourism at Lampuuk and Lhok'nga, **d** Cement factory

using the COMCOT model. The expected results are to provide an overview of the characteristics of the tsunami hazard along the coast of the study area, facilitate tsunami disaster mitigation efforts, provide information to the community on where to evacuate whenever there is a tsunami alert, and promote the development of plans for future local authorities, such as the setting for a safe location of a tsunami emergency management center (evacuation area and building).

Methodology

Wave generation

A tsunami is a movement of a large volume of water, and a significant source of energy is needed to generate it. Submarine and near coast earthquakes, landslides and volcanic eruptions can initiate tsunami (Power and Leonard 2013). Approximately 80% of all tsunamis worldwide that are observed have been caused by underwater earthquakes (UNISDR 2017), and the main potential sources

of tsunamis in the region of this study are the subduction zones off the west coast of Sumatra (Pribadi et al. 2013). In this study, we limited the wave generator caused by an earthquake and the location of the rupture is closest to the study site, namely, the Aceh-Andaman megathrust fault, as shown in Fig. 2. Wells and Coppersmith developed a method for predicting tsunami parameters based on magnitude, and several regression analyses have been applied to the study of the relationship between magnitude and rupture area (Wells and Coppersmith 1994), as in Eqs. (1) to (3).

$$Log(RLD) = -2.42 + 0.58 * M \tag{1}$$

$$Log(RW) = -1.61 + 0.41 * M \tag{2}$$

$$Log(MD) = -1.84 + 0.29 * M \tag{3}$$

where RLD is subsurface rupture length (km), RW is downdip rupture width (km), M is the magnitude, and MD is maximum displacement (m).

Propagation and inundation

The Cornell Multi-grid Coupled Tsunami Model (COMCOT) was used to simulate tsunami inundation. There are two steps to this numerical model, the first step is tsunami wave generation and the second is to demonstrate the movement of tsunami waves as they travel to the mainland from the epicentre (inundation), using a layered grid structure.

COMCOT implements the shallow water equation's linear and non-linear equations for both spherical and cartesian coordinate systems (Wang 2009). Because the height of a tsunami in the deep sea is less than the depth of the ocean, the shallow water linear equation for spherical coordinates was utilised, and the equations are as in Eqs. (4) to (7).

$$\frac{\partial \eta}{\partial t} + \frac{1}{R\cos\varphi}\left\{\frac{\partial P}{\partial \psi} + \frac{\partial \eta}{\partial \psi}(\cos\varphi Q)\right\} = 0 \tag{4}$$

$$\frac{\partial P}{\partial t} + \frac{gh}{R\cos\varphi}\frac{\partial P}{\partial \psi} - fQ = 0 \tag{5}$$

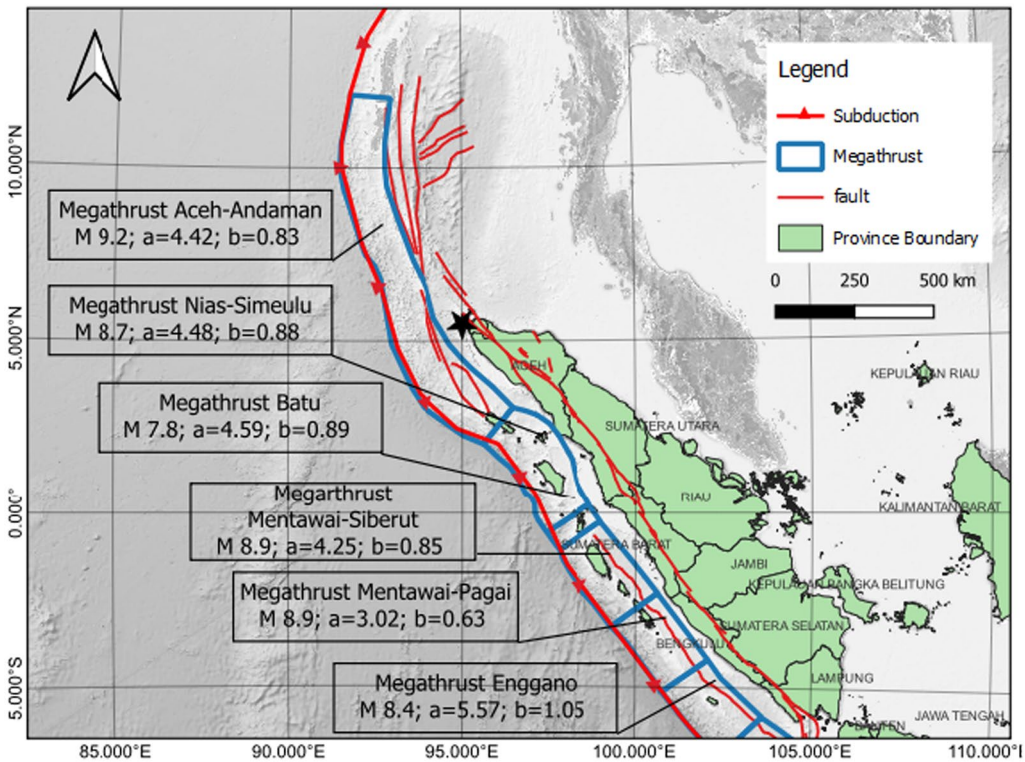

Fig. 2 Fault Segmentation and M_{maks} of Subduction around Sumatra Island, Indonesia (Tim Pusat Studi Gempa Nasional 2017); the black star indicates the study area

$$\frac{\partial Q}{\partial t} + \frac{gh}{R}\frac{\partial \eta}{\partial \psi} + fP = 0 \tag{6}$$

$$f = \Omega \sin \varphi \tag{7}$$

When the tsunami waves approach the coastal area, a non-linear equation is used. The shallow water non-linear equations in Eqs. (8) to (12) for the spherical coordinate system were utilised in COMCOT:

$$\frac{\partial \eta}{\partial t} + \frac{1}{R\cos\varphi}\left\{\frac{\partial P}{\partial \psi} + \frac{\partial}{\partial \psi}(\cos\varphi Q)\right\} = 0 \tag{8}$$

$$\frac{\partial P}{\partial t} + \frac{1}{R\cos\varphi}\frac{\partial}{\partial \psi}\left\{\frac{P^2}{H}\right\} + \frac{1}{R}\frac{\partial}{\partial \varphi}\left\{\frac{PQ}{H}\right\} + \frac{gH}{R\cos\varphi}\frac{\partial \eta}{\partial \psi} - fQ + F_x = 0 \tag{9}$$

$$\frac{\partial Q}{\partial t} + \frac{1}{R\cos\varphi}\frac{\partial}{\partial \psi}\left\{\frac{PQ}{H}\right\} + \frac{1}{R}\frac{\partial}{\partial \varphi}\left\{\frac{Q^2}{H}\right\} + \frac{gH}{R}\frac{\partial \eta}{\partial \psi} + fP + F_y = 0 \tag{10}$$

$$F_x = \frac{gn^2}{H^{\frac{7}{3}}}P\left(P^2 + Q^2\right)^{1/2} \tag{11}$$

$$F_y = \frac{gn^2}{H^{\frac{7}{3}}}Q\left(P^2 + Q^2\right)^{1/2} \tag{12}$$

In Eqs. (4) to (12), η denotes the elevation of the water's surface; (P,Q) denotes the volume fluxes in X (West–East) direction and Y (South–North) direction; (φ,ψ) denotes the longitude and latitude of the Earth; R denotes Earth's radius; g denotes the gravitational acceleration; h denotes the water depth. Term f is the Coriolis force coefficient; Ω is the rotation rate of the Earth; H is the total water depth, and H = η + h; (F_x, F_y) specifies bottom friction in the X and Y directions; n is the Manning's roughness coefficient, and g is the gravitational acceleration.

The Aida approach was used for the validation. (AIDA 1978; Komata 2019; Tursina et al. 2021). Comparisons between observations and computations were validated using variables flow depth and inundation distance. The equations are as follows.

$$K_i = \frac{x_i}{y_i} \tag{13}$$

$$\text{Log } K = \frac{1}{n}\sum_{i=1}^{n}\log K_i \tag{14}$$

$$Logk = \sqrt{\frac{1}{n}\sum_{i=1}^{n}(\log K_i)^2 - (\log K)^2} \tag{15}$$

where n is the number of points, K and k are the Aida coefficient, K represents the geometric mean, and k represents the standard deviation. Variables x_i and y_i are the observed and computed variables. The geometric standard deviation indicates the variance in correspondence between the tsunami observation and the computation value. The results were classified as a good agreement if $k \leq 1.60$ and the range of K number from 0.8 to 1.2 (Takeuchi et al. 2005). The less the geometric standard deviation (k), the more closely the computation value matches the observation.

Probabilistic tsunami hazard assessment (PTHA)

Probabilistic Tsunami Hazard Assessment (PTHA) is a fundamental tools to assess the community's threats (Geist and Parsons 2006; Sørensen et al. 2012; Horspool et al. 2014; Omira et al. 2015). PTHA is an analysis that can be carried out to estimate the long-term hazard in an area that is likely to be affected by a tsunami, including the uncertainty of the information in the assessment (Grezio et al. 2017). PTHA is also essential in supporting evidence of decision-making related to risk mitigation activities (Mulia et al. 2020).

Adapting information from the probabilistic seismic hazard assessment introduced by Cornell (1968), PTHA estimates the rate of exceedance of a given tsunami height H relative to the tsunami height h, which can be written as:

$$\gamma(H \geq h) = \sum_{i=1}^{n_s} \nu_i \sum_{j=1}^{n_m} P\left(H \geq h | m_j\right) P\left(M_i = m_j\right), \tag{16}$$

where n_s is the total number of i tsunami sources, n_m is a number of considered magnitude m with an interval of j. In this calculation, the limit of the earthquake magnitude is from the magnitude m_{min} to the largest magnitude m_{max} with an interval of 0.2. Variable ν shows the level of occurrence of earthquakes with magnitude M, which is equal to or greater than $m_{min,}$, which can be calculated using the Gutenberg-Richter method (Gutenberg and Richter 1944) in Eq. (17).

$$\nu = 10^{a - bm_{min}}, \tag{17}$$

where the values of a and b are constants that are calculated based on the occurrence of earthquakes in the study area. In this study, the values of a and b were obtained

based on the results of the study by the team of Pusat Studi Gempa Nasional (PuSGeN) (Tim Pusat Studi Gempa Nasional 2017). Values a and b for the study area were taken, based on the location of the Aceh-Andaman megathrust, which are $a=4.42$ and $b=0.83$, as shown in Fig. 2.

The probabilities that all of the magnitude ranges in Eq. (17) are derived from the frequency distribution equation of Gutenberg-Richter (F_M),

$$F_M(m) = \frac{1 - 10^{-b(m-m_{min})}}{1 - 10^{-b(m_{max}-m_{min})}} \tag{18}$$

$$PM = mj = FMmj + 0.5\Delta m - FMmj - 0.5\Delta m \tag{19}$$

where Δm is the magnitude interval. The probability that the tsunami height H exceeds the tsunami height h based on the magnitude m in Eq. (19) can be written as

$$P(H \geq h|m) = 1 - \Phi\left\{\frac{\ln(h) - \overline{ln(H)}}{\beta}\right\} \tag{20}$$

where Φ represents the cumulative normal distribution function, $\overline{ln(H)}$ is the median of the log tsunami heights of all models,$\beta = \ln(\kappa)$, κ is the Aida coefficient (AIDA 1978). Value β is included in the calculation because of the uncertainty associated with the tsunami simulation and the tsunami fault/source (Mulia et al. 2020).

The results of PTHA are developed into hazard curve, hazard map, and probability maps (Horspool et al. 2014). Hazard curves are the starting point for all maps, which means that each map is a derivative product that may be used to offer information on a variety of elements of tsunami risk. The hazard curve shows the expected tsunami height on the coast during a given return period. These maps are useful for determining the size of a tsunami that is expected to hit an area within a certain period of time. Probability maps define the probability of exceeding the tsunami height at a given location, and this probability is related to the threat threshold in the TEWS system. This is useful for determining the annual probability of issuing a tsunami warning and, more specifically, for prioritising locations that are most likely to be affected by a tsunami, and pose risks to human life. These maps can be used to compare the risk posed by different tsunami sources.

Data preparation

Multiple levels of the numerical simulation were employed. In the first step, a basic waveform was made around the source. In order to pursue the next step of the tsunami wave generator, the necessary input data for the bathymetry of the Indian Ocean up to the research region were used. These data were gathered from GEBCO (General Bathymetric Chart of the Ocean). The grid size of these data was one minute (or 1856 km) (International Hydrographic Organization (IHO) and (IOC)). In this model, earthquakes are the source of the wave generator. The model is based on seven different earthquake magnitude scenarios, ranging from 8.0 to 9.2 with 0.2 interval. The Mw 9.2 earthquake is about the same size as the 2004 tsunami in the Andaman Sea (Koshimura et al. 2009).

The next step in the modelling of tsunamis was to simulate the movement of tsunami waves as they travel from the epicentre to the mainland (inundation). This level requires more comprehensive bathymetric, topography, and land use data (Manning's n values). Bathymetry data with a precision of 6 arc seconds were collected from BATNAS (National Bathymetry Data, Indonesia). High resolution topography data with spatial resolution of 0.27-arcsecond or 8.35 m, as obtained from DEMNAS (National Digital Elevation Model; DEM, Indonesia) which can be accessed through http://tides.big.go.id (Pusat Jaring Kontrol Geodesi dan Geodinamika). Land use data obtained from the Ministry of Environment and Forestry (MOEF) of the Republic of Indonesia (http://appgis.menlhk.go.id/) (Direktorat Jenderal Planologi Kehutanan). The land use at the study area consisted of forest/plantation (n = 0.035), housing/build-up area (n = 0.040), open land/rice field (n = 0.02), and ponds (n = 0.017).

Result

Earthquake scenarios

The wave generation is based on seven earthquake scenarios with earthquake magnitudes in the range of Mw 8.0 to 9.2 with an interval of 0.2, as shown in Table 1. The rapture parameters for the 9.2 earthquake magnitude are based on the 2004 earthquake conditions (Koshimura et al. 2009). The rapture parameter for the Mw 8.0 to 9.0 scenario is calculated using the Wells and Coppersmith method (Wells and Coppersmith 1994). The location of the wave generator is along the Sumatra Andaman subduction zone. The location of the epicentre is predicted to be at the location of the earthquake in 2004. The complete fault parameters for all scenarios are shown in Table 1.

Sea level movement at the source of the tsunami for various scenarios is shown in Fig. 3. The red colour indicates a positive or rising wave, and the blue colour indicates a negative or down wave. The initial condition of the smallest tsunami wave occurs in scenario Mw 8.0, as shown in Fig. 3a, with a positive wave height of + 3.40 m, a negative wave height of − 1.21 m, and which forms a water column of 165 km in length. The largest wave

Table 1 Tsunami scenario based on fault parameters

Scenarios	Mw	L (Km)	W (km)	Dis (m)	Strike (°)	Dip (°)	Rake (°)	Epicenter		Total L (km)	Depth, D (Km)	References
								Long.	Lat.			
1	8.00	165.00	46.77	8.0	329.0	4.6	110	93.32	4.48	165.00	10	Wells and Coppersmith (1994)
2	8.20	216.77	56.49	8.0	329.0	5.9	110	93.32	4.48	216.77	10	
3	8.40	283.14	68.23	8.0	329.0	7.4	110	93.32	4.48	283.14	10	
4	8.60	125.00	80.00	9.4	335.0	15	90	93.32	4.48	305.00	10	
		180.00	80.00	9.4	340.0	15	90	92.87	5.51		10	
5	8.80	200.00	100.00	11.9	323.0	15	90	94.4	3.03	650.00	10	
		125.00	100.00	11.9	335.0	15	90	93.32	4.48		10	
		180.00	100.00	11.9	340.0	15	90	92.87	5.51		10	
		145.00	100.00	11.9	340.0	15	90	92.34	7.14		10	
6	9.00	200.00	120.00	12.0	323.0	15	90	94.4	3.03	775.00	10	
		125.00	120.00	12.6	335.0	15	90	93.32	4.48		10	
		180.00	120.00	12.1	340.0	15	90	92.87	5.51		10	
		145.00	120.00	7.0	340.0	15	90	92.34	7.14		10	
		125.00	120.00	7.0	345.0	15	90	91.88	8.47		10	
7	9.20	200.00	150.00	14.0	323.0	15	90	94.4	3.03	1155.00	10	Koshimura et al. (2009)
		125.00	150.00	12.6	335.0	15	90	93.32	4.48		10	
		180.00	150.00	15.1	340.0	15	90	92.87	5.51		10	
		145.00	150.00	7.0	340.0	15	90	92.34	7.14		10	
		125.00	150.00	7.0	345.0	15	90	91.88	8.47		10	
		380.00	150.00	7.0	7.0	15	90	91.9	11		10	

conditions occurred in the Mw 9.2 scenario with a positive wave height of + 9378 m and a negative wave height of − 3.507 m, with a fault condition of 6 parts, and which formed a water column of 1155 km; see Fig. 3g. Initial tsunami conditions for the Mw 8.2 to 9.0 scenario are shown in Fig. 3b–f. Based on this fault source, the tsunami waves will propagate to the west coast area of Aceh Besar.

Validation

The tsunami height and inundation distance variables were validated using the 2004 tsunami caused by the Mw 9.2 earthquake magnitude. The fault parameter for this earthquake for validation is referred to Koshimura et al. (2009). NOAA established 172 observation points for the 2004 tsunami height along the study area. The overlay between observed flow depth from NOAA, digitized inundation limit, and flow depth obtained from computation using COMCOT for the 2004 tsunami is shown in Fig. 4b–d. The inundation limit line was determined by comparing aerial photos taken before and after the tsunami (June 2004 and January 2005). Thirty points of inundation distance from the coastline to the inundation limit were determined along the coast for this study. Several point locations were still overestimated and underestimated in comparison to the observed ones for the flow depth comparison (Fig. 5). Although the computation of the tsunami inundation distance is substantially closer to the digitized tsunami limit (Fig. 6).

Using the Aida method for validation, it was found that the results of the tsunami modeling in this study were a good agreement for flow depth from NOAA and inundation distance. The Aida coefficient comparing observed and computation for flow depth is $K = 1139$ and a value of $k = 1585$. Validation for the inundation distance variable also has a good agreement with $K = 1036$ and $k = 1130$. (Table 2).

Flow depth and inundation area

Figure 7 shows a tsunami simulation using COMCOT for seven earthquake scenarios.The picture shows a map of tsunami inundation and tsunami height (blue to red colour). The most comprehensive and highest inundation area occurred due to the tsunami scenario with a magnitude of Mw 9.2, as shown in Fig. 7 (Mw 9.2). The maximum inundation distance for this scenario occurs in the Lhoknga sub-district, with an inundation distance of 6 km, and a maximum tsunami height of 13 m. Regarding the Leupung district, this area experienced the highest tsunami hit, reaching 20 m, but the inundation distance was not too great, because there are hills near the coast. The tsunami arrival time for this location is less

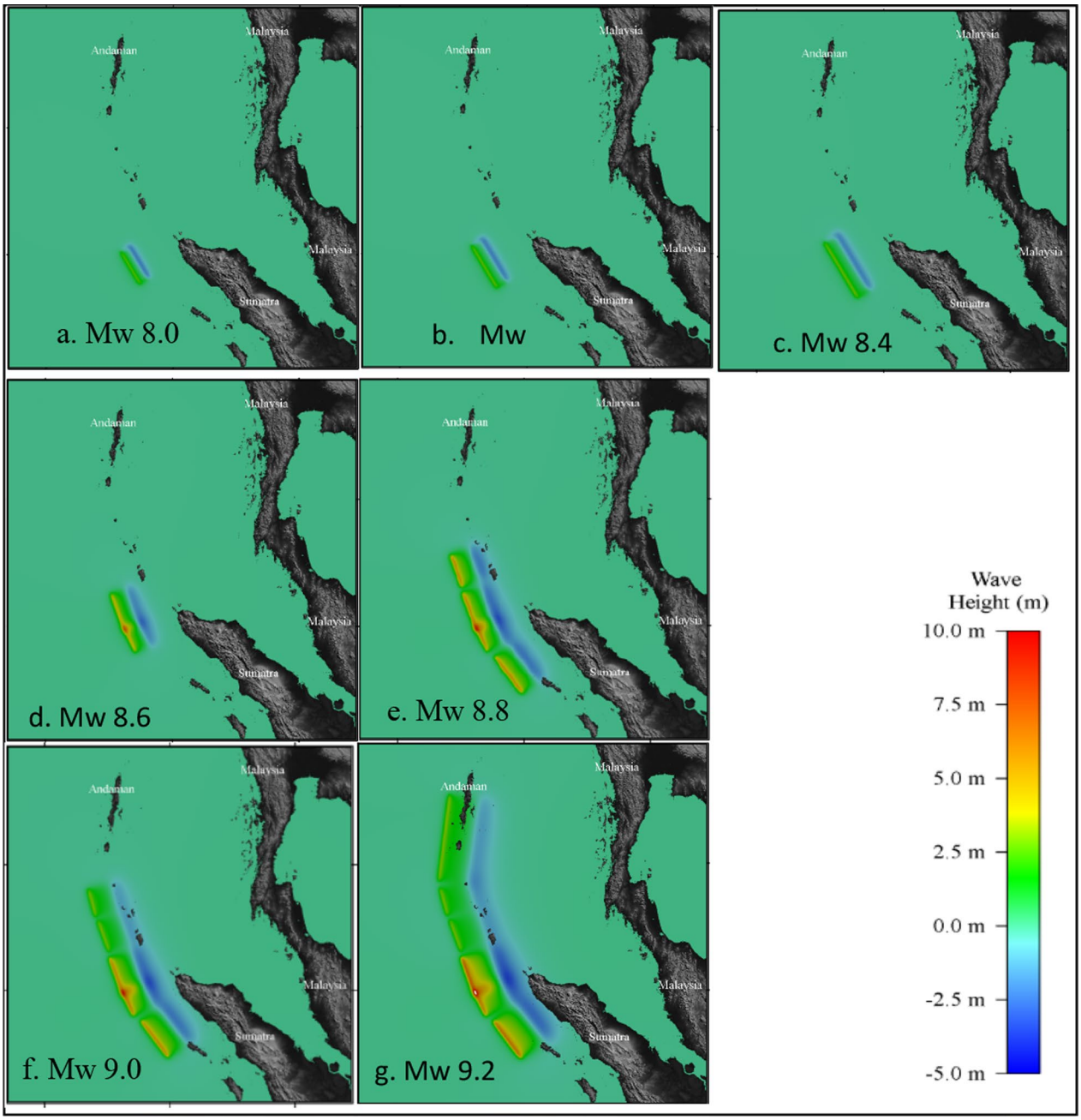

Fig. 3 Initial tsunami height with seven scenarios of earthquake magnitude, from Mw 8.0 (**a**) to Mw 9.2 (**g**)

than 25 min (Syamsidik et al. 2015). Due to the conditon of tsunami arrival time and longest inundation distance, evacuation buildings are recommended for the area in Lhoknga and Leupung, in order to reduce the risk of casualties. It is necessary to arrange a hilly area close to the beach, so that it can be used as an evacuation area, or for vertical evacuation. The maximum flow depth can be used to determine the minimum elevations that are needed for vertical evacuation within the inundation zone, and for the design of buildings that would resist hydrostatic demands. Inundation maps for other scenarios can be seen in Fig. 7 (Mw 8.0–9.2).

In determining PTHA, the observation point is defined as shown in Fig. 8a. There are 397 observation points located 50 m from the shoreline, with a distance of 200 m between points. The tsunami height at the observation location is shown in Fig. 8b. For the Mw 8 scenario, the average tsunami height along the coast,

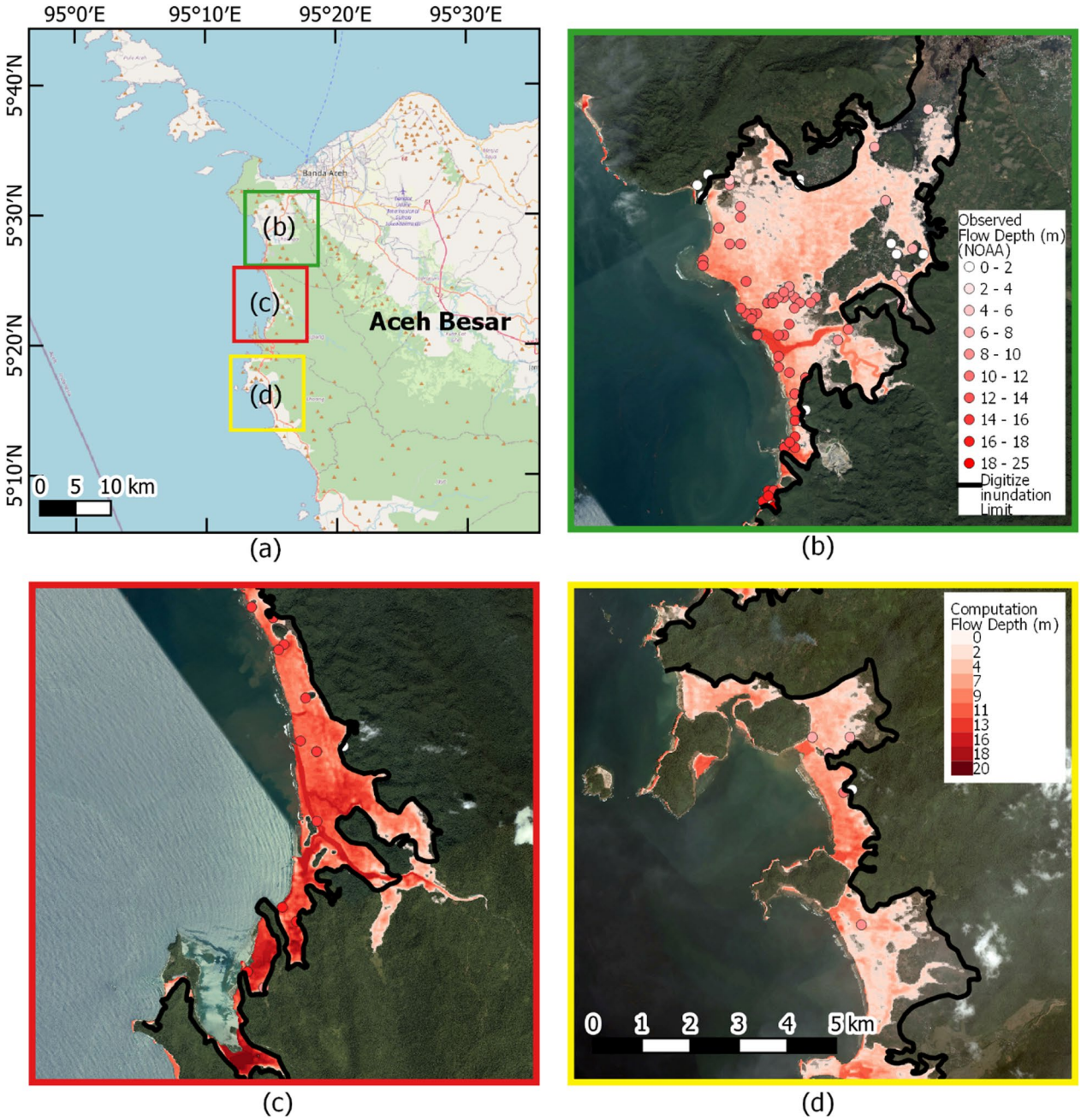

Fig. 4 **a** Location of observed flow depth from NOAA and digitizing tsunami limit. **b**, **c** overlay between NOAA observed data, digitized tsunami limit after tsunami 2004 (January 2005) from Google Earth, and computation flow depth for the 2004 tsunami

or at the observation point, is generally 3.94 m. From the seven simulation scenarios, the maximum tsunami height at the observation point is + 18.1 m, which is located in Leupung, and is caused by the Mw 9.2 scenario. The figure also shows the average tsunami height along the coast. The average tsunami for Mw 8.0 scenario is 3.94 m. The average tsunami height continues to increase as the tsunami magnitude increases. The highest average tsunami height in the Mw 9.2 scenario is as high as 12.18 m.

Hazard level

The tsunami threat is located along the west coast of Aceh Besar District. There are 397 hazard location points within 50 m of the observed coastline. The hazard curve

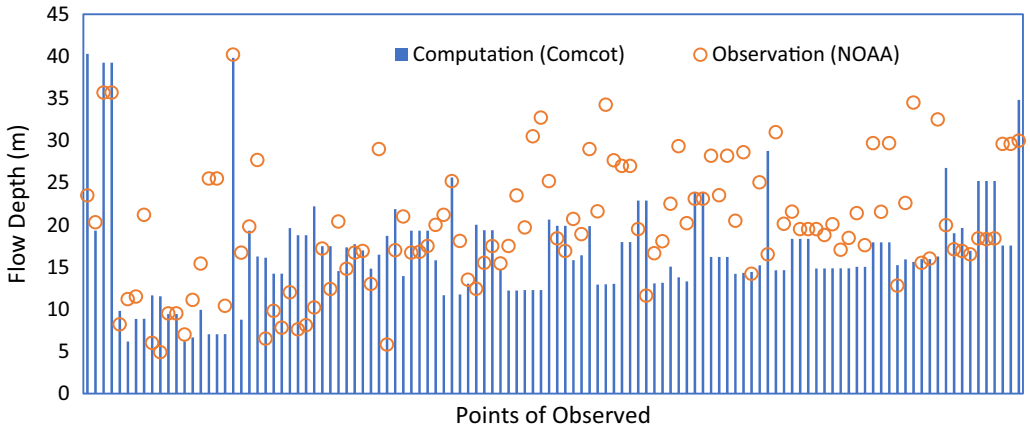

Fig. 5 Computation and observed flow depth from NOAA

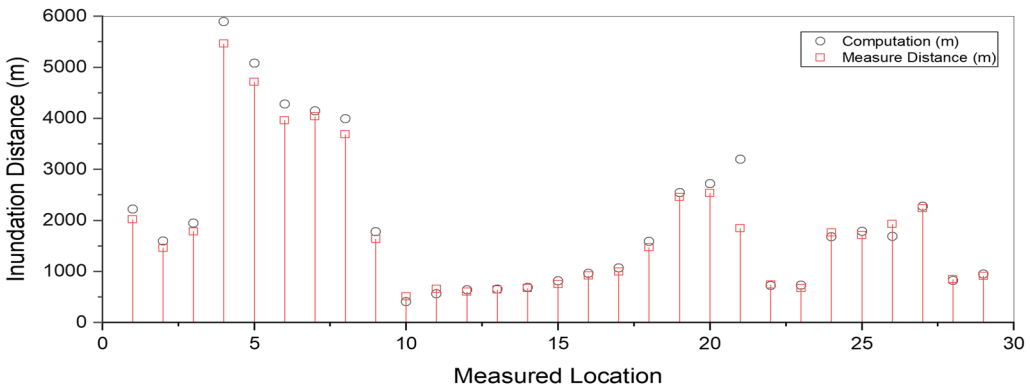

Fig. 6 Comparison between computation and measured inundation distance

Table 2 Validation of tsunami height and inundation distance

Aida coefficient	Required range	Result			
		Flow depth (NOAA) (NOAA)		Inundation distance	
Geometric mean (K)	K (0.8 ≤ K ≤ 1.2)	1.139	Good Agreement	1.036	Good agreement
Geometric standard deviation (k)	k (k ≤ 1.6)	1.585	Good Agreement	1.130	Good agreement

for the study area is shown in Fig. 9, and the light blue colour line indicates the hazard curve for every point in the study area. For the west coast of Aceh Besar, the flow depth on the coast may exceed 1–5 m, with an exceedance probability rate close to ~ 0.01, or 100-year return period. The annual probability is getting smaller for tsunami heights greater than 5 m. For example, with a tsunami height of 12 m, the annual probability is 0.001 (1000-year return period). The high exceedance probability rate for a tsunami height of up to 5 m on the west coast of Aceh Besar is due to the proximity of the earthquake source, and the potential for a large earthquake magnitude (up to Mw 9.2).

The tsunami hazard map was calculated for return periods of 200, 500, and 1000 years. From Hazard map with a period of 200 years (Fig. 10a), shows that the lowest tsunami height is 4.4 m (dark blue colour), and the maximum estimated tsunami height is 13 m, located in the coastal area of Lhoknga. On a hazard map with a return period of 500 years (Fig. 10b), tsunami heights ranged from 6.5 to 16.2 m. The hazard map with a return period of 1000 years is that with the most significant risk in this

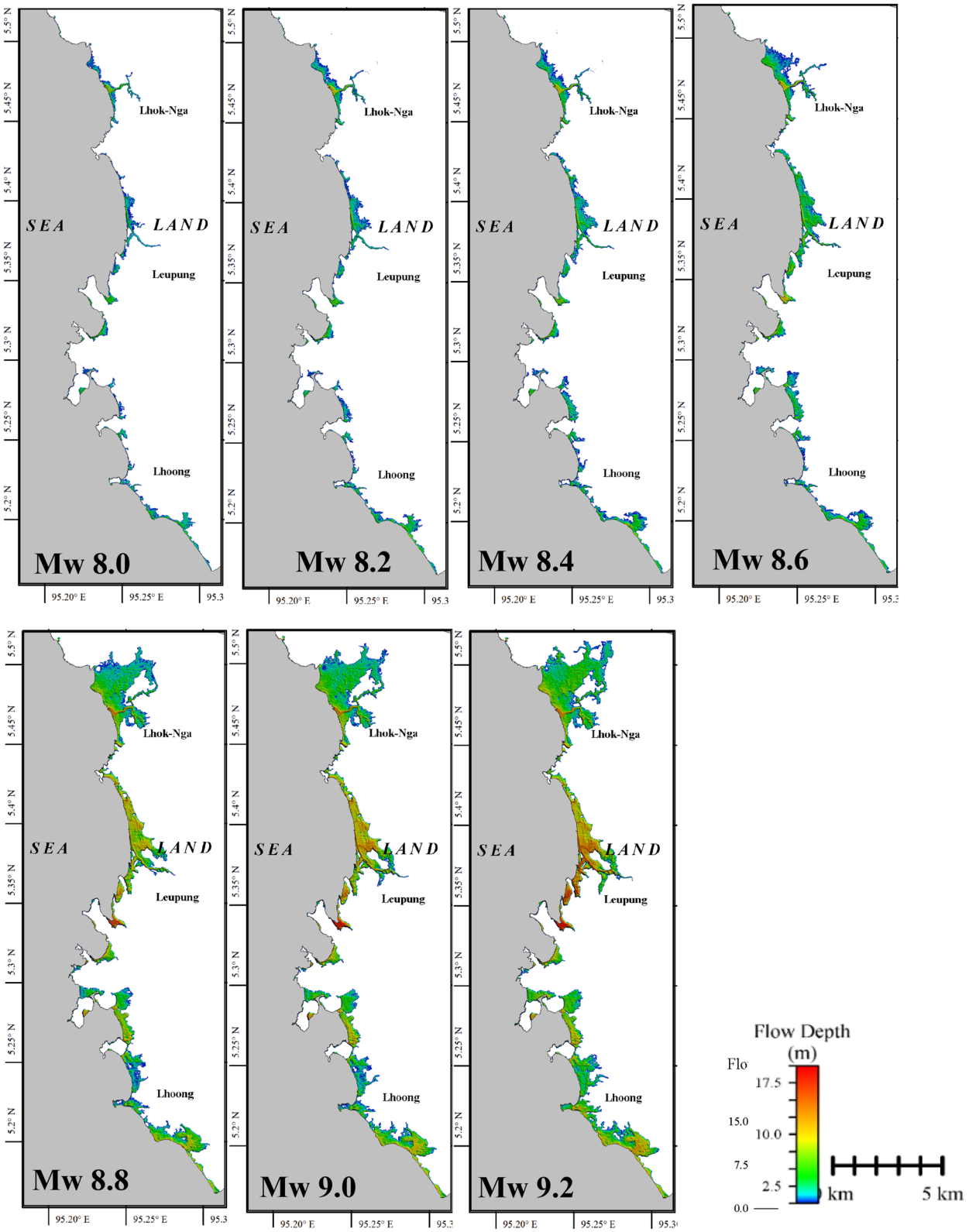

Fig. 7 Inundation map for seven scenarios with earthquake magnitudes from Mw 8.0 to Mw 9.2

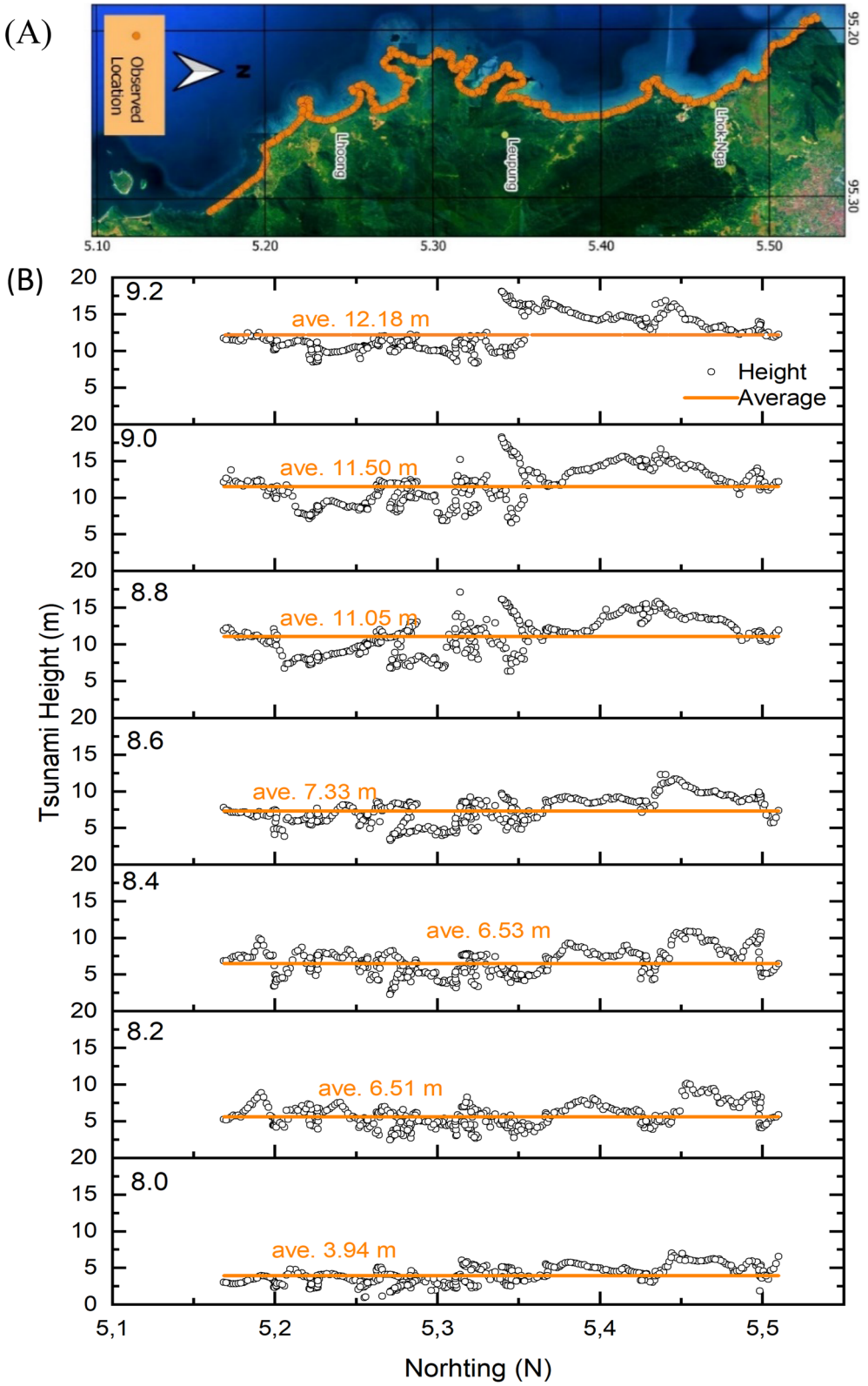

Fig. 8 **A** Observation points located 50 m from the shoreline (orange colour), **B** Tsunami height at the observation point for scenarios Mw 8.0 to Mw 9.2 (orange line indicates average tsunami height/flow depth)

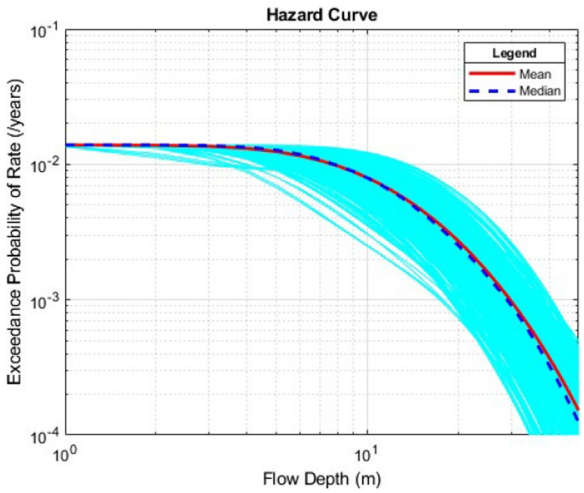

Fig. 9 Tsunami hazard curve at each observation point (blue), including mean and median graphs for the study area

study (Fig. 10c). The tsunami height range for this return period is 9–21 m. From the three calculated periods, it can be seen that the area with a greater tsunami hazard is in the northern part of the west coast of Aceh Besar, compared to the southern region. This is influenced by the location of the earthquake, which is closer to that location. It should also be noted that sites within the bay have a higher risk of being hit by a tsunami, compared to areas in front to them (for example, the locations marked with the black star in Fig. 10c.

Discussion

In the case of a magnitude 9.2 earthquake, or one that was analogous to the tsunami that struck Aceh in 2004, tsunami height at the shoreline reached 18.1 m. This tsunami will cause a maximum inundation distance of up to 2 kms in Lhoknga. The inundation distance in this study was similar to the earlier study (Syamsidik et al. 2019). The cause of tsunamis in this area is generally due to undersea earthquakes. The historical tsunami in the Aceh and Andaman areas shows that an earthquake caused the tsunami in this area with a return period of 500–600 years caused by the movement of the Sunda megathrust. (Sieh 2007; Natawidjaja 2015).

This study shows that the heights of the tsunami increase from south to north of the study area. Maximum tsunami heights that occur for periods of 200, 400 and

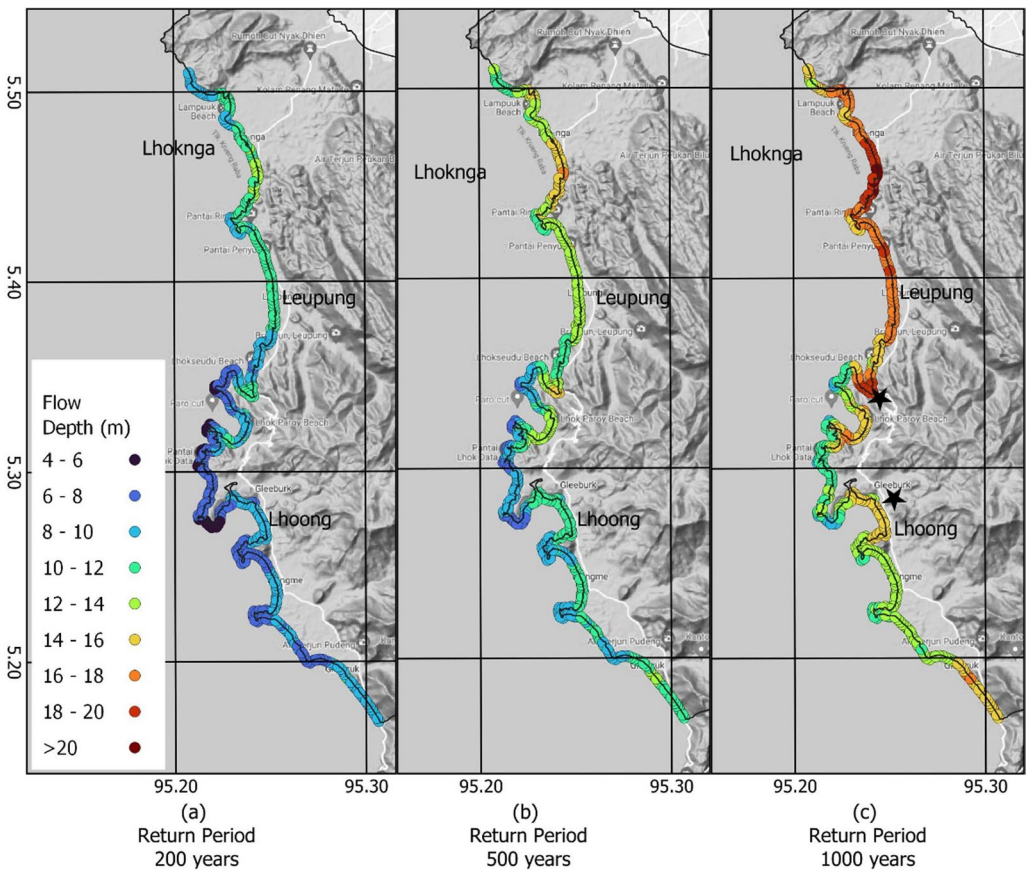

Fig. 10 Tsunami Hazard Map for 200, 400, and 1000-year return periods at the observation site

1000 years are 12.9 m, 16.3 m and 20.8 m, respectively. The resulted tsunami heights were generated by earthquakes where their sources are located around the Aceh-Andaman Megathrust segment, near to the west coast of Aceh Besar. Consequently, the estimated tsunami arrical times for this area are relatively short. These research results once again confirm the staggering challenges of the disaster managers to cope with such extreme condition (Mulia et al. 2020).

Notwithstanding with the elucidated results, this study also acknowledges some limitations that may inspire further researches on this topic. Although historical data showed that tsunamis in this area were caused by undersea earthquakes (Sieh 2007; Natawidjaja 2015), it is also necessary to consider the possibility of a tsunami caused by other factors such as landslide. The earthquake scenarios in this study were limited to 7 scenarios. Therefore, it is also necessary to model other possible scenarios to see the impact on this study area. Furthermore, in long-term period, impacts of sea level rise coupled with tsunami propagation will give different results which have not been considered in this study (Tursina et al. 2021). With some of the existing limitations, this study has described a hazard map for tsunami height in a number of recurrence periods. This study is expected to be useful for further researchs in the framework of tsunami mitigation in other tsunami prone areas.

Conclusions

This study develops a tsunami inundation map based on high-resolution (8.35 m) topographic data, and PTHA for the west coast of Aceh Besar, Indonesia, which consists of three sub-districts, namely, Lhoknga, Leupung, and Lhoong. The maximum inundation distance is 6 km, placed in a flat area in the Lhoknga (residential and tourism area) with a flow depth of up to 13 m. The maximum flow depth is 20 m from ground level in the Leupung area. The southern part of Leupung beach to Lhoong beach is dominated by a short coastline followed by steep hills, which results in a shorter inundation distance than the Lhoknga area, which has a gentler sloping of the area along the coast. Regarding the flat areas in Lhoknga and northern Leupung, these are where there is a risk of longer inundation distances, which is prioritised for establishing vertical evacuation areas or tsunami evacuation buildings. Average flow depths at the shoreline for exceedance probability of 0.01 or 100-year return periods is 1 to 5 m; and for return period 1000 years, the flow depth is 12 m. The areas within the bay has a higher risk of being hit by a tsunami, compared to areas in front of them. Because of the possibility of tsunamis in the future, ongoing tsunami drills and tsunami education are required to ensure that people do not forget how to respond appropriately in the event of a tsunami.

Author contributions

Sy developed frameworks for probabilistic tsunami hazards analysis for this region and write some sections in this article. Ib performed PTHA analysis as well as writing most of sections in this article. Az and Mu guided process of analysis and reviewed the results presented. Ab provided access to computational facilities. Mu developed source codes for computing PTHA. All authors read and approved the final manuscript.

Funding

The authors receive a research grant from LPDP of the Ministry of Finance of Indonesia, under Research Grant RISPRO INVITASI I with title "SupeRISKa: Decision Support System for Disaster Risk Financing and Insurance based on Hazards Characteristics 2021–2024" Contract No. PRJ-103/LPDP/2021. Authors also receive support from the Centre for Research and Community Services (LPPM) Universitas Syiah Kuala for this research under Scheme PUU Penugasan 2022.

Declarations

Competing interests

We, authors in this article, declare that we do not have any relevant financial or non- financial competing interests to disclose.

Author details

[1]Doctoral Program, School of Engineering, Universitas Syiah Kuala, Banda Aceh 23111, Indonesia. [2]Tsunami and Disaster Mitigation Research Center (TDMRC), Universitas Syiah Kuala, Jl. Hamzah Fansuri No. 8, Banda Aceh 23111, Indonesia. [3]Department of Civil Engineering, Politeknik Negeri Lhokseumawe, Lhokseumawe 24301, Indonesia. [4]Department of Civil Engineering, Faculty of Engineering, Universitas Syiah Kuala, Banda Aceh 23111, Indonesia.

Received: 20 October 2022 Accepted: 4 March 2023
Published online: 20 March 2023

References

AIDA I (1978) Reliability of a tsunami source model derived from fault parameters. J Phys Earth 26:57–73. https://doi.org/10.4294/jpe1952.26.57

Al'ala M, Syamsidik S, Rasyif T, Fahmi M (2015) Numerical simulation of ujong seudeun land separation caused by the 2004 Indian ocean tsunami, Aceh-Indonesia. Sci Tsunami Hazards 34:159–172

Allin CC (1968) Engineering seismic risk analysis. Bull Seismol Soc Am 58:1583–1606

Badan Pusat Statistik (BPS) (2019) Kabupaten Aceh Besar Dalam Angka 2019. Aceh Besar

Direktorat Jenderal Planologi Kehutanan Direktorat Jenderal Planologi Kehutanan. http://appgis.menlhk.go.id/. Accessed 23 Jun 2021

Frucht E, Salamon A, Rozelle J et al (2021) Tsunami loss assessment based on Hazus approach – The Bat Galim, Israel, case study. Eng Geol 289:106175. https://doi.org/10.1016/j.enggeo.2021.106175

Geist EL, Lynett PJ (2014) Source processes for the probabilistic assessment of tsunami hazards. Oceanography 27:86–93. https://doi.org/10.5670/oceanog.2014.43

Geist E, Parsons T (2006) Probabilistic analysis of tsunami hazards*. Nat Hazards 37:277–314. https://doi.org/10.1007/s11069-005-4646-z

Goff JR, Terry JP (2012) Living with natural hazards in the Asia–Pacific region. Geol Soc London 361(1):1–2. https://doi.org/10.1144/SP361.1

Grezio A, Babeyko A, Baptista MA et al (2017) Probabilistic tsunami hazard analysis: multiple sources and global applications. Rev Geophys 55:1158–1198. https://doi.org/10.1002/2017RG000579

Gusman AR, Tanioka Y, Takahashi T (2012) Numerical experiment and a case study of sediment transport simulation of the 2004 Indian Ocean tsunami in Lhok Nga, Banda Aceh, Indonesia. Earth, Planets Sp 64:3. https://doi.org/10.5047/eps.2011.10.009

Gutenberg B, Richter CF (1944) Frequency of earthquakes in California*. Bull Seismol Soc Am 34:185–188. https://doi.org/10.1785/BSSA0340040185
Horspool N, Pranantyo I, Griffin J et al (2014) A probabilistic tsunami hazard assessment for Indonesia. Nat Hazards Earth Syst Sci 14(3105–3122):2. https://doi.org/10.5194/nhess-14-3105-2014
Ibrahim, Syamsidik, Azmeri, et al (2022) Investigating characteristics of tsunami hazards for west coast of Aceh Besar district, Indonesia. E3S Web Conf 340:01005. https://doi.org/10.1051/e3sconf/202234001005
International Hydrographic Organization (IHO), (IOC) Intergovernmental Oceanographic Commission General Bathymetric Chart of the Ocean (GEBCO). In: UNESCO. https://www.gebco.net/
Jihad A, Muksin U et al (2020) Coastal and settlement typologies-based tsunami modeling along the northern Sumatra seismic gap zone for disaster risk reduction action plans. Int J Disaster Risk Reduct 51:101800. https://doi.org/10.1016/j.ijdrr.2020.101800
Komata R (2019) Evaluation of tsunami scouring on subsea pipelines. IOP Conf Ser Earth Environ Sci 326(1):012010. https://doi.org/10.1088/1755-1315/326/1/012010
Koshimura S, Oie T, Yanagisawa H, Imamura F (2009) Developing fragility functions for tsunami damage estimation using numerical model and post-tsunami data from banda aceh, Indonesia. Coast Eng J 51:243–273. https://doi.org/10.1142/S0578563409002004
Li L, Qiu Q, Huang Z (2012) Numerical modeling of the morphological change in Lhok Nga, west Banda Aceh, during the 2004 Indian Ocean tsunami: understanding tsunami deposits using a forward modeling method. Nat Hazards 64:1549–1574. https://doi.org/10.1007/s11069-012-0325-z
Liu Y, Ren Y, Wen R, Wang H (2021) Probabilistic tsunami hazard assessment for the southeast coast of China: consideration of both regional and local potential sources. Pure Appl Geophys 178:5061–5084. https://doi.org/10.1007/s00024-021-02878-w
Martínez C, Cienfuegos R, Inzunza S et al (2020) Worst-case tsunami scenario in Cartagena Bay, central Chile: challenges for coastal risk management. Ocean Coast Manag. https://doi.org/10.1016/j.ocecoaman.2019.105060
Mulia IE, Ishibe T, Satake K et al (2020) Regional probabilistic tsunami hazard assessment associated with active faults along the eastern margin of the Sea of Japan. Earth, Planets Sp. https://doi.org/10.1186/s40623-020-01256-5
Natawidjaja DH (2015) Siklus mega-tsunami di wilayah aceh-andaman dalam konteks sejarah. Ris Geol Dan Pertambangan. https://doi.org/10.14203/risetgeotam2015.v25107
NOAA National Geophysical Data Center / World Data Service: NCEI/WDS Global Historical Tsunami Database
Okal E (2015) The quest for wisdom: lessons from 17 tsunamis, 2004–2014. Philos Trans A Math Phys Eng Sci. https://doi.org/10.1098/rsta.2014.0370
Omira R, Baptista MA, Matias L (2015) Probabilistic tsunami hazard in the northeast atlantic from near- and far-field tectonic sources. Pure Appl Geophys 172:901–920. https://doi.org/10.1007/s00024-014-0949-x
Ontowirjo B, Paris R, Mano A (2013) Modeling of coastal erosion and sediment deposition during the 2004 Indian Ocean tsunami in Lhok Nga, Sumatra, Indonesia. Nat Hazards 65:1967–1979. https://doi.org/10.1007/s11069-012-0455-3
Paris R, Wassmer P, Sartohadi J et al (2009) Tsunamis as geomorphic crises: lessons from the December 26, 2004 tsunami in Lhok Nga, West Banda Aceh (Sumatra, Indonesia). Geomorphology 104:59–72. https://doi.org/10.1016/j.geomorph.2008.05.040
Power W, Leonard GS (2013) Tsunami. In: Bobrowsky PT (ed) Encyclopedia of natural hazards. Springer Netherlands, Dordrecht, pp 1036–1046. https://doi.org/10.1007/978-1-4020-4399-4_56
Pribadi S, Afnimar PNT, Ibrahim G (2013) Characteristics of earthquake-generated tsunamis in Indonesia based on source parameter analysis. J Math Fundam Sci 45:189–207. https://doi.org/10.5614/j.math.fund.sci.2013.45.2.8
Pusat Jaring Kontrol Geodesi dan Geodinamika Pusat Jaring Kontrol Geodesi dan Geodinamika. http://tides.big.go.id
Rasyif T, Syamsidik S, Al'ala M, Fahmi M (2016) Numerical simulation of the impacts of reflected tsunami waves on Pulo Raya Island during the 2004 Indian Ocean tsunami. J Coast Conserv. https://doi.org/10.1007/s11852-016-0464-6
Satake K, Nishimura Y, Putra PS et al (2013) Tsunami source of the 2010 Mentawai, Indonesia Earthquake inferred from Tsunami field survey and waveform modeling. Pure Appl Geophys 170:1567–1582. https://doi.org/10.1007/s00024-012-0536-y
Sieh KE (2007) The sunda megathrust — past, present and future. J Earthq Tsunami 01:1–19. https://doi.org/10.1142/S179343110700002X
Sihombing F, Torbol M (2017) Probabilistic tsunami hazard assessment through large scale simulations BT - 14th international probabilistic workshop. In: Taerwe L, Proske D (eds) Caspeele R. Springer International Publishing, Cham, pp 285–295
Siregar Novita T (2016) Analisis perubahan garis pantai dan tutupan lahan pasca tsunami pantai lhoknga, kecamatan lhoknga, kabupaten aceh besar. Progr Stud Kehutan USU
Sørensen MB, Spada M, Babeyko A et al (2012) Probabilistic tsunami hazard in the Mediterranean Sea. J Geophys Res Solid Earth. https://doi.org/10.1029/2010JB008169
Suppasri A, Maly E, Kitamura M et al (2021) Cascading disasters triggered by tsunami hazards: a perspective for critical infrastructure resilience and disaster risk reduction. Int J Disaster Risk Reduct 66:102597. https://doi.org/10.1016/j.ijdrr.2021.102597
Syamsidik et al (2015) Development of accurate tsunami estimated times of arrival for tsunami-prone cities in Aceh, Indonesia. Int J Disaster Risk Reduct 14:403–410. https://doi.org/10.1016/j.ijdrr.2015.09.006
Syamsidik et al (2016) Numerical simulations of impacts of the 2004 Indian Ocean tsunami on coastal morphological changes around the ulee lheue bay of aceh. Indonesia J Earthq Tsunami 11:1740005. https://doi.org/10.1142/S179343111740005X
Syamsidik et al (2019) Numerical simulations of the 2004 Indian Ocean tsunami deposits' thicknesses and emplacements. Nat Hazards Earth Syst Sci 19:1265–1280. https://doi.org/10.5194/nhess-19-1265-2019
Takeuchi T, Murashima Y, Imamura F et al (2005) Verification of tsunami run-up height records of Meiji Sanriku Tsunami and Showa Sanriku Tsunami on the coast of Iwate Prefecture using numerical simulation. Hist Earthq 20:155–163
Tim Pusat Studi Gempa Nasional (2017) Peta Sumber Dan Bahaya Gempa Indonesia Tahun 2017
Tonini R, Di Manna P, Lorito S et al (2021) Testing tsunami inundation maps for evacuation planning in Italy. Front Earth Sci 9:1–19. https://doi.org/10.3389/feart.2021.628061
Tursina et al (2021a) Coupling sea-level rise with tsunamis: projected adverse impact of future tsunamis on Banda Aceh city, Indonesia. Int J Disaster Risk Reduct 55:102084. https://doi.org/10.1016/j.ijdrr.2021.102084
UNISDR (The United Nations International Strategy for Disaster Reduction) (2013) From shared risk to shared value –the business case for disaster risk reduction
UNISDR (2017) Tsunami hazard and risk assessment. Words into Action Guidel Natl Disaster Risk Assess 1–9
Wang X (2009) COMCOT user manual ver. 1.7. Cornell Univ 6:1–59
Wells D, Coppersmith K (1994) New empirical relationships among magnitude, rupture length, rupture width, rupture area, and surface displacement. Bull Seismol Soc Am 84:974–1002

Publisher's Note